Design of cascaded diffractive phase elements for three-dimensional multiwavelength optical interconnects

Xuegong Deng and Ray T. Chen

Microelectronics Research Center, Department of Electrical and Computer Engineering, The University of Texas at Austin, Austin, Texas 78758

Received March 24, 2000

We propose a novel design method that incorporates multiple-layer relief profiles of diffractive phase elements to implement integrated operations on the incident beams according to their wavelengths. We demonstrate simultaneous wavelength-division demultiplexing, arbitrary (even random) wavelength shuffling or routing, spatial focusing, and other manipulations of multiwavelength beams, such as irradiance profile shaping, with design examples for applications in three-dimensional optical interconnects. © 2000 Optical Society of America

OCIS codes: 050.1970, 200.4650, 060.0060, 330.6180, 130.0130, 100.3190.

Diffractive optical elements, especially diffractive phase elements (DPE's) with inherently high diffraction efficiencies, have many distinctive features that make them potentially useful for integrated and miniaturized optics. It is possible to implement such optical functions as beam shaping, beam splitting, focusing, wave-front correction, achromatic aberration correction, switching, pulse temporal-domain shaping,[1–3] and wavelength-division demultiplexing (WDDM) in one element.[4] A number of algorithms for designing a DPE for single-wavelength operations have been reported.[5–8] There are several methods for designing DPE's to generate distinct fan-out patterns working at two wavelengths or beam splitting at multiple wavelengths.[4,9–11] However, none of the existing methods provides a satisfying solution to the problem of designing complicated multiple optical wavelength interconnects (MOWI's) in three-dimensional (3-D) settings.[12] In this Letter we report an algorithm for designing multiple-layer DPE's for certain MOWI's in layered 3-D settings (Fig. 1).

In Fig. 1, optical fields with amplitudes $U_{i,0}(\lambda_w, \mathbf{r})$, $\mathbf{r} \equiv (x, y)$, at wavelength λ_w, $w = 1, 2, 3, \ldots, N_W$, emitted from source S (arrays of laser diodes or light-emitting diodes), overlap on the first DPE. They are diffracted through the succeeding L-layer DPE's and targeted to the desired region, T. In general, a 3-D region T is associated with the constraints of the desired target irradiance distributions, $I_t(\lambda_w, \mathbf{r}) = |U_t(\lambda_w, \mathbf{r})|^2$. The method of diffraction of these fields by the DPE's can be generalized as follows: Let the optical fields on the front surface of the lth DPE be $U_{i,l}(\lambda_w, \mathbf{r})$, $l = 1, 2, 3, \ldots, L$. Each field will experience a different phase delay $\phi_l(\lambda_w, \mathbf{r})$ introduced by the microstructured surface profile $h_l(r)$ just behind the DPE layer. The field amplitudes on the surfaces of the next succeeding DPE's can be expressed as

$$U_{i,l+1}(\lambda_w, \mathbf{r}) = U_{0,l}(\lambda_w, \mathbf{r}) = \mathcal{P}\{U_{i,l}(\lambda_w, \mathbf{r}) T_l(\lambda_w, \mathbf{r}) \exp[\, j\phi_l(\lambda_w, \mathbf{r})]\},$$

$$\phi_l(\lambda_w, \mathbf{r}) = \frac{2\pi}{\lambda_w}[n_r(\lambda_w) - n_s(\lambda_w)] h_l(\mathbf{r}) = k_w{}^{(e)} h_l(\mathbf{r}), \quad (1)$$

where $\mathcal{P}\{\}$ is the propagation operator, $j \equiv \sqrt{-1}$, $T_l(\lambda_w, \mathbf{r}) \approx 1$ is the amplitude transmission of the DPE, and $n_r(\lambda_w)$ and $n_s(\lambda_w)$ are the indices of refraction of the relief structure and of the surrounding medium [usually air, $n_s(\lambda_w) \approx 1$]. Our goal has been to find a set of realizable $h_l(\mathbf{r})$ under the constraints of given $U_{i,0}(\lambda_w, \mathbf{r})$, $|U_t(\lambda_w, \mathbf{r})|$ and the distances from surface P_1 to the targets in area T. We provide a general algorithm with which to attack the problem as well as a detailed application that we believe offers a unique way to deal with the 3-D MOWI's.

The new algorithm extends previous studies of the design of single-layer diffractive optical elements that work with monochromatic waves.[13] In Ref. 13 the authors presented an iteration algorithm based on the approximation of weak-phase deviations (WPDA's). Applying that approximation to the 3-D MOWI structure, we use the corresponding relief profile, $h_l{}^{(n+1)} = h_l{}^{(n)} + \delta h_l{}^{(n)}(\mathbf{r})$, at the $(n + 1)$th iteration. Suppose that a sufficiently good approximation were obtained in the nth iteration that made $h_l{}^{(n+1)}(\mathbf{r})$, $|\delta h_l{}^{(n)}(\mathbf{r})| \ll |h_l{}^{(n)}(\mathbf{r})|$, satisfying Eqs. (1); one would have

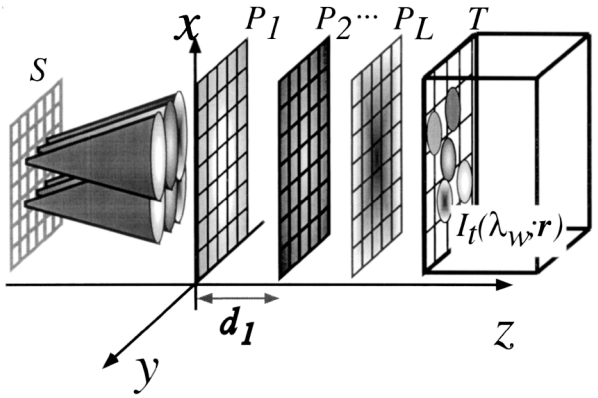

Fig. 1. Schematic illustration of multiwavelength optical interconnects in 3-D space. Beams at several wavelengths from an array of lasers or light-emitting diodes at S overlap on the first DPE at P_1. Several layers of DPE's can be used to achieve almost any distribution $I_t(\lambda_w, \mathbf{r})$ in target region T.

0146-9592/00/141046-03$15.00/0

$$U_{i,l}(\lambda_w, \mathbf{r})\exp[\, jk_w{}^{(e)}h_l{}^{(n)}(\mathbf{r})][1 + jk_w{}^{(e)}\delta h_l{}^{(n)}(\mathbf{r})] \approx \mathcal{P}^{-1}[U_{0,l}(\lambda_w, \mathbf{r})], \quad w = 1, 2, 3, \ldots, N_W, \quad (2)$$

where $\mathcal{P}^{-1}[\,]$ is the inverse propagation operator. To ensure that the relief profiles have real values and to avoid possible singularity and branch cuts, we may construct the iteration for $h_l(\mathbf{r})$ as

$$h_l{}^{(n+1)}(\mathbf{r}) = h_l{}^{(n)}(\mathbf{r}) + \frac{1}{\sum_{w=1}^{N_W} \epsilon_{l,w}{}^{(n)}} \times \sum_{w=1}^{N_W} \epsilon_{l,w}{}^{(n)} \mathcal{I}\left\{\frac{\mathcal{P}^{-1}[U_{0,l}{}^{(n)}(\lambda_w, \mathbf{r})]}{k_w{}^{(e)}U_{i,l}{}^{(n)}(\lambda_w, \mathbf{r})\exp[\, jk_w{}^{(e)}h_l{}^{(n)}(\mathbf{r})]}\right\}, \quad (3)$$

in which $\epsilon_{l,w} = \| \mathcal{P}[U_{i,l}{}^{(n)}(\lambda_w, \mathbf{r})] - U_{0,l}{}^{(n)}(\lambda_w, \mathbf{r}) \| / \| U_{0,l}{}^{(n)}(\lambda_w, \mathbf{r}) \|$ is the rms error of the approximated surface profile for wavelength λ_w at the lth layer, $U_{i,l}{}^{(n)}$ may be replaced with a modified function of the incident beams after some regularization,[13] and $\mathcal{I}\{\}$ stands for the imaginary part of a function. Notice that the superscripts that indicate the iteration number are included in Eq. (3) because both $U_{i,l}(\lambda_w, \mathbf{r})$ and $U_{0,l}(\lambda_w, \mathbf{r})$ will be updated in each iteration, as explained in the algorithm below. Other required operations on the relief profiles, such as taking thresholds, filtering, quantization, and optimization, can easily be integrated because this algorithm acts directly on $h_l(\mathbf{r})$.

To deal with the initialization process of the field amplitudes on the intermediate $(L - 1)$ layers, for simplicity we have adopted the following procedure:

1. Initialize all the $h_l(\mathbf{r})$ with uniform random numbers in $[0, \lambda_p]$, where $\lambda_p = 1/N_W \sum_{w=1}^{N_W} \lambda_w$.
2. Begin the propagation operation on the incident fields and obtain the field distributions on all the succeeding planes P_l, $l = 1, 2, 3, \ldots, L$, and target region T by using Eqs. (1). Record the irradiance profiles on the intermediate planes.
3. Perform backpropagation with WPDA, starting from the last DPE plane P_L:

(a) Replace the irradiance profiles of the fields in the target region with the constraints $I_t(\lambda_w, \mathbf{r}) = |U_t(\lambda_w, \mathbf{r})|^2$. It is then possible to find the relief profile on the Lth plane by means of the WPDA [Eqs. (3)].

(b) Repeat the above step for the remaining DPE's from the $(L - 1)$th layer backward to the first layer, using the irradiance profiles obtained in Step 2 as constraints. The surface relief profiles, $h_l(\mathbf{r})$, $l = L - 1, L - 2, \ldots, 1$, can easily be updated.

4. Iterate step 2 and step 3 for a given number of loops or until the result exceeds some predefined error criteria.

We benefit also from a recent study of fast chirp transforms for computing the propagation processes $\mathcal{P}[\,]$ in a Fresnel region that has uniform formulas in one-, two-, three-, or even higher-dimensional spaces (if one needs to include the temporal characteristics of the diffraction).[14] Furthermore, the window size and the sampling rate on each layer may be freely chosen. It is important, however, to remember that the constraints must be physical. One can almost certainly satisfy the physical constraints by increasing the number of DPE layers.[15] The minimum number of DPE layers depends on the number of degrees of freedom of the optical system and may not be easily determinable in general.[16]

To demonstrate the effectiveness of this algorithm as simply as possible, we applied the algorithm to the 3-D optical interconnects in Fig. 1, but we illustrate only the one-dimensional result. We chose fused silica as the material used for the DPE's. The spacing between DPE's, $d_l = z_{l+1} - z_l$, the sampling numbers N_l, and the window size R_l of each DPE are all assumed to be the same, and T is taken as a plane located at $z_T = z_L + d_1$. We design a set of DPE's that simultaneously accomplish WDDM, arbitrary (including random) wavelength shuffling or routing (WSR), focusing, and beam shaping on the target plane. All incident beams and their distributions on the targets are Gaussian. Their amplitudes are $A_{s,w}\exp\{-[(x - x_{s,w})/\sigma_s]^2\}$, $s = i, t$; $w = 1, 2, \ldots, N_W = 4$. In our simulation, $N_l = 500$, $d_l = 3.0 \times 10^4$ μm, $\sigma_i = 0.35R_i = 1260.7$ μm, $\sigma_0 = 82.3$ μm, $x_{i,w} = 0$, $x_{t,w} = 4\sigma_0[w - (N_W + 1)/2]$, $w = 1 \ldots 4$. We randomly shuffle the order of the incident wavelengths λ_w to emulate arbitrary routing of the multiwavelength beams. Their ideal profiles $I_{i,t}(\lambda_w, \mathbf{r})$, turn out to be of the order of $\lambda_{1\ldots4} = 0.827$, 0.980, 0.903, 0.750 μm, respectively, from left to right on plane T (Fig. 2). The results, quantitatively evaluated, include three quantities: the energy confinement factor $E_{c,m}$, the cross talk $X_{m,n}$ (energy leakage from channel m to $n \neq m$), and the profile rms $\epsilon_{t,m}$. The former two quantities are defined as

$$E_{c,m} = R_{m,m}/C_m, \qquad X_{m,n} = R_{m,n}/R_{m,m}, \qquad n \neq m, \quad (4)$$

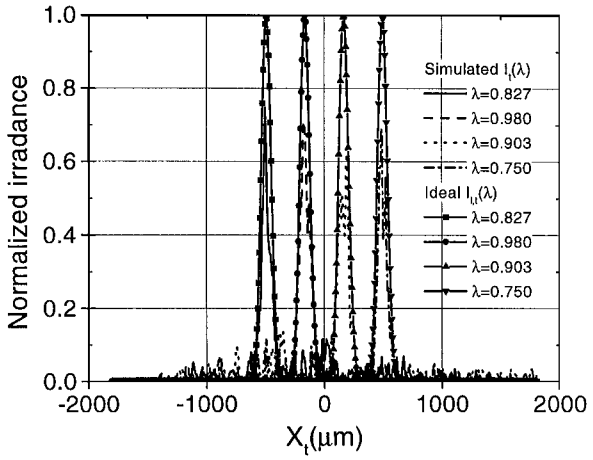

Fig. 2. Irradiance distributions on the target plane of the two-layered 3-D DPE's for simultaneous WDDM, random WSR, spatial focusing, and shaping of the irradiance profiles of the multiple-wavelength incident beams.

Table 1. Summary of Quantitative Evaluation of the Integrated Operations: Energy Confinement Factor $E_{c,m}$, Profile rms $\epsilon_{t,m}$, and Cross Talk $X_{m,n}$, $m, n = 1 \ldots 4$, and $n \neq m$

	Target Number			
	1	2	3	4
λ_m (μm)	0.827	0.980	0.903	0.750
$E_{c,m}$	0.547	0.628	0.502	0.579
$\epsilon_{t,m}$	0.703	0.589	0.707	0.704
$X_{m,n}$				
$n = 1$		0.0171	0.0878	0.0798
$n = 2$	0.0603		0.0130	0.0293
$n = 3$	0.0182	0.0164		0.0130
$n = 4$	0.0539	0.0452	0.0104	

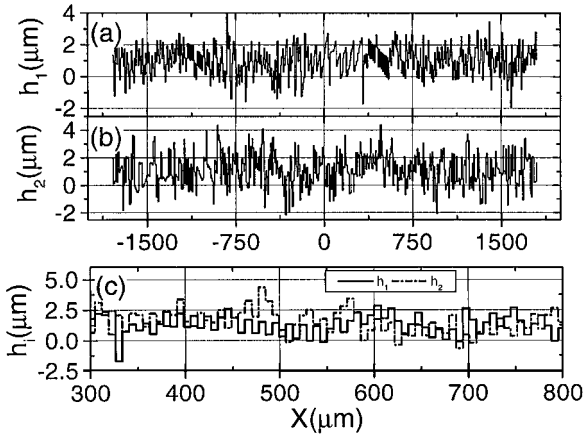

Fig. 3. Surface profiles of (a) the first DPE and (b) the second DPE. Notice the feature size of the reliefs in the magnified profile (c).

in which

$$R_{m,n} = \frac{\int_{x_{t,n}-\sigma_0}^{x_{t,n}+\sigma_0} I_t(\lambda_m, \mathbf{r})\mathrm{d}x\mathrm{d}y}{\int_{-\infty}^{+\infty} I_t(\lambda_m, \mathbf{r})\mathrm{d}x\mathrm{d}y},$$

$$C_m = \frac{\int_{x_{t,m}-\sigma_0}^{x_{t,m}+\sigma_0} I_{i,t}(\lambda_m, \mathbf{r})\mathrm{d}x\mathrm{d}y}{\int_{-\infty}^{+\infty} I_{i,t}(\lambda_m, \mathbf{r})\mathrm{d}x\mathrm{d}y}. \quad (5)$$

A summary of these quantities appears in Table 1; for corresponding surface-relief profiles, see Fig. 3. Simulations with other wavelength orders ($N_W!$ unique sequences for N_W wavelengths in a one-dimensional WSR problem) show similar or better results. This is a fairly compact MOWI structure. Its performance compares favorably with results achieved so far (see, e.g., Ref. 4). This two-layer MOWI simultaneously performs WDDM, arbitrary WSR, focusing, and beam shaping. The cross talks among channels are less than 10%. With more layers, the performance is better. The relief structures for this MOWI can be realized in mass production with current microelectronics technology. Other engineering details, for example, the required alignment tolerance of the MOWI structure, may also be considered in this transform-based algorithm. One may directly generate DPE's that are insensitive to fluctuations of the incident fields' amplitude, phase, or both, as demonstrated in Ref. 17.

In brief, we have presented a novel method for the design of multilayer three-dimensional multi-optical-wavelength interconnects. To provide an application example, we demonstrated the successful solution of a set of realizable relief profiles for integrating wavelength-division demultiplexing, arbitrary wavelength shuffling–routing, focusing, and beam shaping into a compact multiple optical wavelength interconnect system. We expect to provide the details of other, more-complex applications in future publications.

The authors thank Barbara Cavanagh for proofreading the manuscript of this Letter. This study is partly supported by the Ballistic Missile Defense Organization, the U.S. Air Force Office of Scientific Research, the Defense Advanced Research Projects Agency, the U.S. Army Space Defense and Missile Command, 3M, Lightpath, and the Texas State Advanced Technology Program. R. T. Chen's e-mail address is raychen@uts.cc.utexas.edu.

References

1. For example, H. P. Herzig, ed., *Micro-optics: Elements, Systems, and Applications* (Taylor & Francis, Bristol, UK, 1997).
2. T. Glasers, S. Schröter, and H. Bartelt, Opt. Lett. **23,** 1933 (1998).
3. K. Takasago, M. Takekawa, M. Suzuki, K. Komori, and F. Kannari, IEEE J. Sel. Top. Quantum Electron. **4,** 346 (1998).
4. B. Dong, G. Zhang, G. Yang, B. Gu, S. Zeng, D. Li, Y. Chen, X. Cui, and H. Liu, Appl. Opt. **35,** 6859 (1996), and references therein.
5. R. W. Gerchberg and W. O. Saxton, Optik (Stuttgart) **35,** 237 (1972).
6. J. R. Fienup, Opt. Eng. **19,** 297 (1980).
7. G. Zhou, Y. Chen, Z. Wang, and H. Song, Appl. Opt. **38,** 4281 (1999).
8. J. R. Fienup, J. Opt. Soc. Am. A **16,** 1831 (1999).
9. I. M. Barton, P. Blair, and M. R. Taghizadeh, Opt. Express **1,** 54 (1997), http://epubs.osa.org/opticsexpress, and references therein.
10. J. Bengtsson, Appl. Opt. **37,** 2011 (1998).
11. T. R. M. Sales and D. H. Raguin, Appl. Opt. **38,** 3012 (1999).
12. C. Tocci and H. J. Caulfield, eds., *Optical Interconnection: Foundations and Applications* (Artech House, Boston, Mass., 1994), Chaps. 2, 4, 7, and 9.
13. X. Deng, Y. Li, D. Fan, and Y. Qiu, Opt. Lett. **21,** 1963 (1996).
14. X. Deng, B. Bipin, J. Gan, F. Zhao, and R. T. Chen, J. Opt. Soc. Am. A **17,** 762 (2000).
15. B. Gu, G. Yang, and B. Dong, Appl. Opt. **25,** 3197 (1986), and references therein.
16. R. Piestun and D. Miller, J. Opt. Soc. Am. A **17,** 892 (2000), and references therein.
17. Y. Chen, D. Li, and Y. Sheng, Appl. Opt. **36,** 568 (1997).